

Emergent traffic jams

Kai Nagel^{1,2,*} and Maya Paczuski^{1,†}¹*Department of Physics, Brookhaven National Laboratory, Upton, New York 11973*²*Center for Parallel Computing ZPR, University of Cologne, 50923 Köln, Germany*

(Received 20 October 1994)

We study a single-lane traffic model that is based on human driving behavior. The outflow from a traffic jam self-organizes to a critical state of maximum throughput. Small perturbations of the outflow far downstream create emergent traffic jams with a power law distribution $P(t) \sim t^{-3/2}$ of lifetimes t . On varying the vehicle density in a closed system, this critical state separates lamellar and jammed regimes and exhibits $1/f$ noise in the power spectrum. Using random walk arguments, in conjunction with a cascade equation, we develop a phenomenological theory that predicts the critical exponents for this transition and explains the self-organizing behavior. These predictions are consistent with all of our numerical results.

PACS number(s): 05.40.+j, 89.40.+k, 05.60.+w

I. INTRODUCTION

Traffic jams are annoying, and they have negative economic impact. For example, it may be noted that in 1990 (1980), 14.8% (16.4%) of the U.S. Gross National Product was absorbed by passenger and freight transportation costs [1]. Rather than increasing the supply of transportation, perhaps by adding new highways or a train-based transit system, or decreasing the demand for transportation, for example by making it more expensive, it is desirable to use existing transportation structures as efficiently as possible. One would, perhaps, want to keep a freeway in the regime of maximum vehicle throughput.

However, it turns out that this regime is not very well understood. Recent numerical simulations using grid based particle models for traffic flow have found indications for a phase transition separating low-density lamellar flow from high-density jammed behavior, where particles either stop moving or move very slowly [2–4]. It has been observed numerically that this transition occurs at or near the point of maximum throughput [5] and that the flow behavior in this region is complex. Continuum fluid-dynamical approaches similarly predict instabilities in this region [6–8], consistent with real world observations [9,10].

Here, we demonstrate that maximum throughput corresponds to a percolative transition for the traffic jams. It occurs at the point where emergent traffic jams are barely able to survive indefinitely. This implies that the intrinsic flow rate for vehicles leaving a jam equals maximum throughput. As a result, the outflow from a large jam (at large distances or times) self-organizes to the maximum throughput critical point. Numerical results show that slow perturbations in the outflow lead to traffic jams, downstream, of all sizes—a particularly simple example of self-organized criticality (SOC) [11]. If the sys-

tem is “driven” with more frequent random perturbations, then the jams will interact. This induces a finite correlation length for the jams and pushes the system off criticality. Similarly, the size of a jam induces a finite size cutoff in its outflow. These considerations imply that traffic in a complicated network is likely to be poised near the critical state determined by the largest jam in the system, and thus susceptible to small perturbations. The characteristic power law associated with the jam lifetimes makes prediction of flow behavior more difficult. Steps that are taken to reduce random fluctuations or perturbations, such as cruise control or automatic car-following systems, in fact, push the traffic network closer to its underlying critical point, thereby making it *more* likely to have large jams.

We study a simplified version of an original discrete model proposed by Nagel and Schreckenberg [4]. This simplification can be described as a “cruise control limit,” since at sufficiently low density all vehicles move deterministically at maximum allowed velocity. This deterministic motion is interrupted by small perturbations at a vanishingly slow rate; i.e., the system is allowed to relax back to a deterministic state before it is kicked again. The emergent traffic jams are the transient response to the perturbation.

In the model, the forward motion of vehicles in a single lane is mimicked by the forward motion of particles on a one-dimensional lattice. The essential features of this model are (a) hard-core particle dynamics; (b) an asymmetry between acceleration and deceleration which, in connection with a parallel update, leads to clumping behavior and jam formation rather than smooth density fluctuations; (c) a wide separation between the time scale for creating small perturbations in the system and the relaxational dynamics, or the lifetime of the jams. The model is studied with both closed and open boundary conditions.

This model exhibits behavior that is characteristic of granular systems [2,12,13–16]. These include phenomena ranging from the rather mundane example of flow of

*Electronic address: kai@zpr.uni-koeln.de

†Electronic address: maya@cmt1.phy.bnl.gov

sand in an hour glass [17] to the large scale structure of the universe [18]. Recent studies of clustering instabilities in one-dimensional many particle systems in which particles interact via inelastic collisions [19] may also be related.

In Sec. II, the traffic model is defined, and its current-density relation is derived. The outflow from a large jam is marked by a power law scaling of the distribution of jam lifetimes with exponent $\frac{3}{2}$. This outflow operates at the point of maximum throughput. Section III presents random walk arguments, which are exact for a version of the model with maximum velocity, $v_{\max}=1$. This theory predicts the critical exponents for the emergent jams. The number of jammed vehicles, n , scales with time as $t^{1/2}$. The space-time jam size (or mass of the jam cluster) $s \sim nt$, and the spatial extent $w \sim n$. On varying the density, ρ , away from the maximum throughput value, ρ_c , the jams have a characteristic lifetime t_{co} , or cutoff, which scales as $t_{\text{co}} \sim (\rho_c - \rho)^2$. It is important to note that jams with $v_{\max} > 1$ are allowed to branch, unlike $v_{\max} = 1$. In Sec. IV, this branching behavior is analyzed in terms of a cascade equation for the size distribution of intervals between parts of the jam. The distribution of interval sizes, x , is predicted to decay as $1/x^2$. This result suggests that the jams are marginally dense and the random walk theory is valid up to logarithmic corrections, e.g., $w \sim t^{1/2} \ln t$. Also, since the jams drift backwards, this distribution of interval sizes gives rise to $1/f$ noise in the power spectrum of local activity. In Sec. V, we present the rest of our numerical results. These results are consistent with our phenomenological theory. In Sec. VI, we discuss the potential relevance of this work to real traffic.

II. THE MODEL

The closed model is defined on a one-dimensional array of length L , representing a single-lane freeway. Each site of the array can be in one of the $v_{\max} + 2$ states: It may be empty, or it may be occupied by one car having an integer velocity between zero and v_{\max} . This integer number for the velocity is the number of sites each vehicle advances during one iteration. Movement is restricted to occur “crash free.” Unless otherwise noted, we choose $v_{\max} = 5$, but any value $v_{\max} \geq 2$ gives the same large scale behavior when lengths are rescaled by a short distance cutoff. This short distance cutoff corresponds roughly to the typical distance required for a vehicle starting at rest to accelerate to maximum velocity.

For every configuration of the model, one iteration consists of the following steps, which are each performed simultaneously for all vehicles (here, the quantity n_{gap} equals the number of empty sites in front of a vehicle).

(i) A vehicle is stationary when it travels at maximum velocity v_{\max} and has free headway: $n_{\text{gap}} \geq v_{\max}$. Such a vehicle just maintains its velocity.

(ii) If a vehicle is not stationary, it is jammed. The following two rules are applied to jammed vehicles.

Acceleration of free vehicles: With probability $\frac{1}{2}$, a vehicle with $n_{\text{gap}} \geq v + 1$ accelerates to $v + 1$, otherwise it keeps the velocity v . A vehicle with $n_{\text{gap}} = v$ just main-

tains its velocity.

Slowing down due to other cars: Each vehicle with $n_{\text{gap}} \leq v - 1$ slows down to n_{gap} : $v \rightarrow n_{\text{gap}}$. With probability $\frac{1}{2}$, it overacts and slows down even further:

$$v \rightarrow \max[n_{\text{gap}} - 1, 0].$$

Movement: Each vehicle advances v sites.

Randomization takes care of two behavioral patterns: (i) Nondeterministic acceleration. This is the source of the scaling behavior of the jam lifetimes. (ii) Overreactions when slowing down. This is considered to be realistic with respect to real traffic [20,21].

While in the original model studied by Nagel and Schreckenberg [4,5], vehicles at v_{\max} slowed down randomly with probability p_{free} , here only the jammed vehicles move nondeterministically. This corresponds to the $p_{\text{free}} \rightarrow 0$ limit, or the “cruise control limit,” of the previous model and completely separates the time scales for perturbing the system and the system’s response.

Our fundamental diagram, or current-density relation, $j(\rho)$, was determined numerically as shown in Fig. 1 for a closed system of size $L = 30\,000$. Starting with a random initial condition with N cars (i.e., $\rho = N/L$) and after discarding a transient period of 5×10^5 iterations, we measured $\langle j \rangle_L(t) = \sum_{i=1}^N v_i / L$ every 2500 time steps up to the 3×10^6 th iteration. Each data point corresponds to the average over current measurements for a single initial condition, with the following exception: When a run becomes stationary (i.e., no more jammed cars in the sense of the definition above), then the future behavior is predictable. In this case, the run is stopped, and the current will be equal to $j_{\text{det}} = \rho v_{\max}$, see below.

For a spatially infinite system, the following results hold: For $\rho < \rho_c$, jams present in the initial configuration are eventually sorted out and the stationary deterministic state is jam free with every vehicle moving at maximum velocity. Thus, in the lamellar regime the current is a linear function of density with slope $v_{\max} = 5$. Lamellar behavior is observed up to a maximum current $j_c(\rho_c)$. For $\rho > \rho_c$, and $\rho < \rho_{\text{det,max}}$ (defined below) the system is

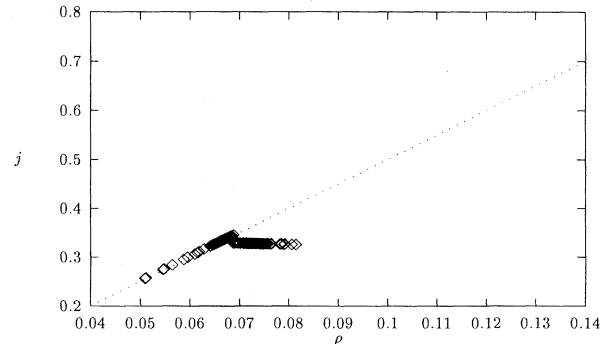


FIG. 1. The fundamental diagram, $j(\rho)$, for $v_{\max} = 5$. The dotted line is valid for deterministic traffic, i.e., when the initial state is prepared such that for each car $n_{\text{gap}} > v_{\max}$ and $v = v_{\max}$. The points are measurement results starting from random initial conditions; each point corresponds to one run of a closed system of length $L = 30\,000$ and an average over 2.5×10^6 iterations.

bistable. Starting from an initial configuration which has many jams, the jams in this case are never sorted out. The steady state is an inhomogeneous mixture of jam free regions and higher density jammed regions. Clearly, these jammed regions decrease the average current in the system. It is possible, nevertheless, to prepare initial configurations that have no jams. Since all motion is deterministic in this state, the steady state will also have no jams and the current will still be a linear increasing function of ρ (the dotted line in Fig. 1). This is possible up to densities of

$$\rho_{\text{det,max}} = \frac{1}{v_{\text{max}} + 1}, \quad (1)$$

leading to a maximum current of

$$j_{\text{det,max}} = \frac{v_{\text{max}}}{v_{\text{max}} + 1}. \quad (2)$$

This clearly is much higher than the current j_c for random initial conditions. It is in this sense that our system is bistable (cf. also [3]). This effect allows us to produce outflows with densities above ρ_c .

Above ρ_c , the current-density relation can be derived by assuming that the system phase separates into jammed regions separated by jam free gaps. The jam free gaps are the outflow of a jam and thus have current $j_c(\rho_c)$, as argued in the next section. Conservation of the number of cars and of volume [22] leads to

$$j = j_c - \frac{(\rho - \rho_c)(aj_c - v_j)}{1 - a\rho_c}, \quad (3)$$

where a is the average number of lattice sites per jammed vehicle, and v_j is the average velocity ($<v_{\text{max}}$) of a jammed vehicle (see [23] for a similar calculation). Thus, the current-density relation is linear both above and below the critical point, as demonstrated in Fig. 1.

The discontinuity in the current at the critical point, as seen in figure, is a finite size effect due to the fact that each point in the figure represents a single initial configuration. In a finite system, there is a finite probability that even a system with supercritical density $\rho > \rho_c$ finds the deterministic state, and then has a current of $j_{\text{det}} > j_c$.

A. The outflow from a jam occurs at maximum throughput

A striking feature of the model is that maximum throughput is selected automatically when the left boundary condition is an infinitely large jam and the right boundary is open. This situation was described for the original model in [5]. An intuitive explanation is that maximum throughput cannot be any higher than the intrinsic flow rate out of a jam. Otherwise the flow rate into a jam would be higher than the flow rate out, and the jam would be stable in the long time limit, thus reducing the overall current. By definition, of course, maximum throughput cannot be lower than this intrinsic flow rate.

In Fig. 2, the cars on the left flow out from a region of high density, where they move with zero velocity. This high density region is not plotted here; only the interface or front separating the high density region and its deterministic outflow is plotted. This is the branched struc-

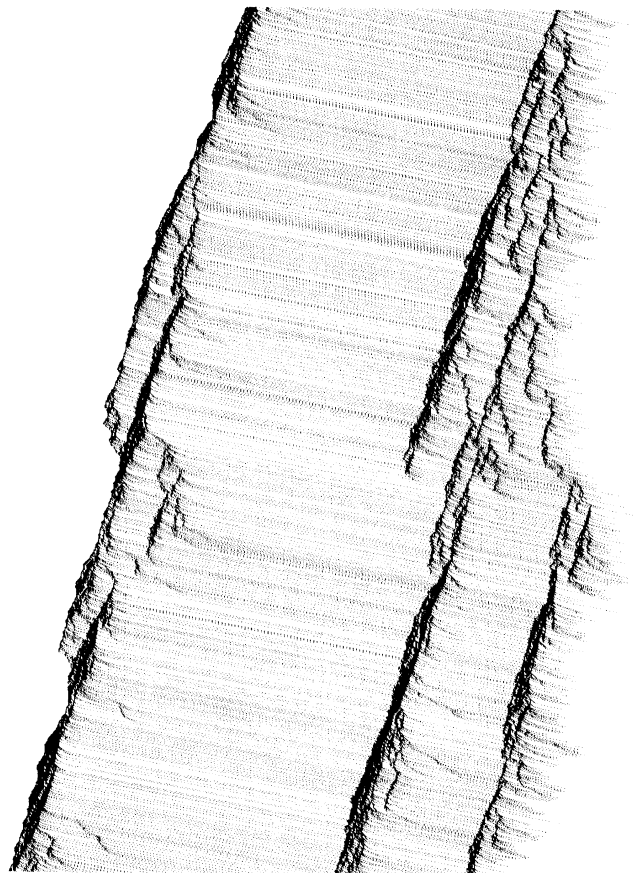


FIG. 2. Outflow from a dense region (left); only the front, or interface, from the dense region is shown as the structure on the left hand side. Dots represent vehicles which move to the right. The horizontal direction is space and the vertical direction (down) is (increasing) time. In the outflow region, an emergent jam is triggered by a small disturbance. This is the structure on the right hand side. “Deterministic” vehicles to the right of the emergent jam are not plotted.

ture on the left hand side of the figure. The vehicles flowing out of the large jam ultimately relax to the deterministic state when they have moved sufficiently far away from the jam.

This feature of maximum throughput selection is characteristic of driven diffusive systems [24–26]. However, in our case the left boundary condition is unusual: the front of the infinite jam drifts backward in time. If the left boundary is fixed in space and vehicles are inserted at velocities less than v_{max} , then the outflow from a jam cannot reach maximum throughput (cf. bottleneck situation in [4,27]). This point warrants further investigation, since it corresponds to the real world observation that disturbances which are fixed in space, such as bottlenecks or on-ramps, lead to much lower throughput downstream than would be possible theoretically [28].

B. Traffic jams in the outflow show self-organized criticality

The outflow situation, as described above, produces deterministic flow asymptotically at large distances. This

means that sufficiently far downstream from the large jam, the jam flow has sorted itself out into deterministic flow. In the deterministic region, one car is randomly perturbed by reducing its velocity to zero. Many different choices for the local perturbation, however, give rise to the same large scale behavior. The perturbed car eventually reaccelerates to maximum velocity. In the meantime, though, a following car may have come too close to the disturbed car and has to slow down. This initiates a chain reaction—the emergent traffic jam.

Figure 2 also shows the first 1400 time steps of such an emergent jam, as the structure on the right hand side of the figure. Qualitatively, the jam clearly shows a tendency to branch with complex internal structure and a fractal appearance [29]. The emergent traffic jams drift backwards; so it is possible for a sufficiently long-lived emergent jam to eventually intersect with the outflow jam interface, on the left in Fig. 2, that is itself becoming broader with time. It is likely that the branching behavior of the emergent jams is the same as the branching behavior of the original jam interface. In this work, however, we do not explicitly study the interface. Contrary to the figure, in the computer code, the interface region to the left and the emergent jam to the right are kept completely separate using methods described in Appendix A.

A jam is sorted out when the number of jammed cars is zero. This defines the lifetime, t , of an emergent traffic jam. In order to obtain statistics for the properties of noninteracting traffic jams, the deterministic outflow is disturbed again, after the previous jam has died out. In our simulations we measure the lifetime distribution, $P(t)$, the spatial extent w of the jam, the number of jammed vehicles n , and the overall space-time size s (mass) of the jam. These properties of the traffic jam are analogous to other branching processes such as directed percolation [36], branching annihilating random walks [31], or nonequilibrium lattice models [32], although the precise behaviors are different. Figure 3 shows 1400 time steps in the middle of the life of a larger jam. Here, vehicles that are stationary are no longer shown; the plot only shows the “particles,” or jammed vehicles, that propagate the disturbance.

For a quantitative treatment, we start by measuring the probability distribution of jams as a function of their lifetime, t . Figure 4 shows that for $t > \approx 100$, this distribution follows a power law,

$$P(t) \sim t^{-(\delta+1)} \quad \text{with } (\delta+1) = 1.5 \pm 0.01, \quad (4)$$

very close to $\delta = \frac{1}{2}$. This figure represents averaged results of more than 65 000 jams.

Here, scaling is observed over almost four orders of magnitude as determined by our *numerically imposed* cutoff: For this figure, if jams survive longer than 10^6 time steps, they are removed from the database. It is very important to note that these emergent jams are precisely critical. Their power law scaling persists up to any arbitrarily large, numerically imposed cutoff. The lifetime distribution is related to the survival probability $P_{\text{surv}}(t)$ by



FIG. 3. Space-time plot of an emergent jam. The horizontal direction is space and the vehicle direction is time, as in Fig. 2. Only vehicles with $v < v_{\text{max}}$, i.e., “particles,” are plotted.

$$P_{\text{surv}}(t) = \int_t^\infty dt' P(t') \sim t^{-\delta} \quad \text{for } \delta > 0. \quad (5)$$

We again emphasize that no external tuning is necessary to observe this scaling behavior. The outflow from the infinite jam self-organizes to the critical state.

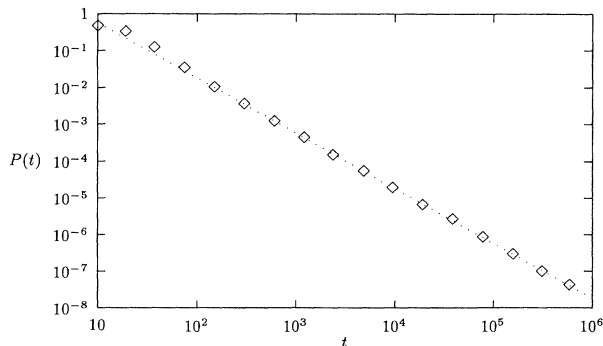


FIG. 4. Lifetime distribution $P(t)$ for emergent jams in the outflow region; average over more than 65 000 clusters (avalanches). The dotted line has slope $\frac{3}{2}$. Numerically imposed cutoff at $t = 10^6$.

III. RANDOM WALK ARGUMENTS FOR CRITICAL BEHAVIOR

It is, perhaps, surprising that such a seemingly complicated structure as shown in Fig. 2 is described by such a simple apparent exponent. Numerically, the exponent $\delta+1$ is conspicuously close to $\frac{3}{2}$, the first return time exponent for a one-dimensional random walk. In fact, for $v_{\max}=1$ this random walk picture is exact, as shown below.

Let us consider a single jam in a large system with $v_{\max}=1$. The vehicles in the jam form a queue, and all of these cars have velocity zero. When the vehicle at the front of the jam accelerates to velocity one, it leaves the jam forever. The rate at which vehicles leave the jam is determined by the probabilistic rule for acceleration. Vehicles, of course, can be added to the jam at the back end. These vehicles come in at a rate which depends on the density and velocity of cars behind the jam. Given the rules for deceleration, the spacing between the jammed cars is zero so the number of cars in the jam, n , is equal to the spatial extent of the jam, w . This contrasts with the branching behavior for $v_{\max} > 1$. The probability distribution, $P(n, t)$, for the number of cars in the jam, n , at time, t , is determined by the following equation:

$$P(n, t+1) = (1 - r_{\text{in}} - r_{\text{out}})P(n, t) + r_{\text{in}}P(n-1, t) + r_{\text{out}}P(n+1, t). \quad (6)$$

Here, the quantities r_{in} and r_{out} are phenomenological parameters that depend on the density behind the jam and the rate at which cars leave a jam. They are independent of the number of cars in the jam. For large n and t , one can take the continuum limit of Eq. (6) and expand to lowest order

$$\frac{\partial P}{\partial t} = (r_{\text{out}} - r_{\text{in}}) \frac{\partial P}{\partial n} + \frac{r_{\text{out}} + r_{\text{in}}}{2} \frac{\partial^2 P}{\partial n^2}. \quad (7)$$

When the density behind the jam is such that the rate of cars entering the jam is equal to the intrinsic rate that cars leave the jam, then the first term on the right hand side vanishes, and the jam queue is formally equivalent to an unbiased random walk in one dimension [33], or the diffusion equation. The first return time of the walk then corresponds to the lifetime of a jam. This leads immediately to the result $P(t) \sim t^{-3/2}$ for the lifetime distribution.

This argument shows that the outflow from an infinite jam is in fact self-organized critical. This can be seen by noting that the outflow from a large jam occurs at the same rate as the outflow from an emergent jam created by a perturbation. This also shows that maximum throughout corresponds to the percolative transition for the traffic jams. Starting from random initial conditions in a closed system, the current at long times is determined by the outflow of the longest-lived jam in the system.

When $r_{\text{in}} = r_{\text{out}}$ one also finds from Eq. (7) that $n \sim t^{1/2}$ and the size of the jam $s \sim nt \sim t^{3/2}$. If the density in the deterministic state is below the critical density ρ_c , then the jams will have a characteristic lifetime, t_{co} , size s_{co} ,

number n_{co} , etc. From Eq. (7), $t_{\text{co}} \sim n_{\text{co}}(r_{\text{out}} - r_{\text{in}})^{-1}$. Assuming that near the critical point $r_{\text{out}} - r_{\text{in}} \sim \rho_c - \rho$, then using $n_{\text{co}} \sim t_{\text{co}}^{1/2}$ leads to

$$t_{\text{co}} \sim (\rho_c - \rho)^{-2}. \quad (8)$$

If the left boundary condition is such that $\rho > \rho_c$, vehicles on average enter the emergent jam at a faster rate than they leave. In this case, there is a finite probability to have an infinite jam, P_∞ , which vanishes as $\rho \rightarrow \rho_c$ as

$$P_\infty \sim (\rho - \rho_c)^\beta. \quad (9)$$

In a closed system, the steady-state density of jammed cars, $\rho_j = \rho - \rho_c$, so that the order parameter exponent is trivially $\beta=1$. From the random walk Eq. (7), and in analogy with other branching processes such as directed percolation [30], P_{surv} follows a scaling form

$$P_{\text{surv}}(t, \Delta) \sim t^{-\delta} f(t \Delta^{v_t}), \quad (10)$$

near the critical point. Here, $\Delta \equiv |\rho - \rho_c|$ and $t_{\text{co}} \sim \Delta^{-v_t}$. From this scaling relation, $\beta = \delta v_t$. For $v_{\max}=1$, $\delta = \frac{1}{2}$, $v_t=2$, and again $\beta=1$.

The number of jammed vehicles, \bar{n} , averaged over all jams, including those that die out, has the scaling form,

$$\bar{n} \sim t^n g(t \Delta^{v_t}). \quad (11)$$

The number of jammed vehicles averaged over surviving jams, scales with a different exponent,

$$n(t) = \bar{n}(t)/P(t) \sim t^{\eta+\delta}. \quad (12)$$

The mapping to the random walk gives $\eta=0$. The cluster width, averaged over surviving clusters, scales as $w \sim t^{1/z}$, and the mapping to the random walk gives $z=2$. The average cluster size $s \sim t^{\eta+\delta+1}$; $s \sim t^{3/2}$ in the random walk case.

In the numerical measurements, we averaged the quantities t =lifetime of the cluster, w =maximum width of cluster during cluster life, n =maximum number of simultaneously jammed vehicles during cluster life, s =total number of jammed vehicles during cluster life.

Our theoretical results should describe the emergent traffic jams not only at $v_{\max}=1$ but also for any $v_{\max} > 1$ as long as the traffic jam itself remains dense. If this is the case, then the dynamical evolution is determined solely by the balance of incoming and outgoing vehicles as described by Eq. (7). The ratio w/n should go to a finite constant at large times if the theory is valid. If the emergent jams break up into a fractal structure, and w/n diverges, internal dynamics must also be included. Since the jams displayed in Figs. 2 and 3 appears branched and at least qualitatively fractal, one might doubt that such a simple theory could describe this behavior. Nevertheless, the close numerical agreement of the lifetime distribution exponent for the SOC behavior suggests the possibility that the random walk theory is a valid description of the branching jam waves.

IV. A CASCADE EQUATION FOR THE BRANCHING JAMS

We now analyze the branching behavior of jams with $v_{\max} > 1$ in terms of a phenomenological cascade equation. A very large emergent jam, at a fixed point in time, consists of small dense regions of jammed cars, which we call subjams, separated by intervals, "holes," where all cars move at maximum velocity. If the jam is dense, then the holes have a finite average size. Otherwise, the jammed vehicles may comprise a fractal with dimension $d_f < 1$. We will consider the subjams to have size one.

Holes between the subjams are created at small scales by the probabilistic rules for acceleration. Each subjam can create small holes in front of it. We will ignore the details of the injection mechanism, and assume that there is a steady rate at which small holes are created in the interior of a very long-lived jam. We also assume that the interior region of a long-lived jam reaches a steady-state distribution of holes sizes. We do not explicitly study the distribution of hole sizes at small scales.

In order to determine the asymptotic scaling of the large holes in the interior of a long-lived jam, it is necessary to isolate the dominant mechanism in the cascade process for large hole generation. This mechanism is the dissolution of one subjam. When one subjam dissolves because the cars in it accelerate to maximum velocity, the two holes on either side of it merge to form one larger hole. Holes at any large scale are created and destroyed by this same process. This mechanism links different large scales together, and we propose that it gives the leading order contribution at large hole sizes. In the steady state, the creation and destruction of large holes must balance. This leads to a cascade equation for holes of size x :

$$\sum_{u=x+1}^{\infty} \langle h(x)h(u-x) \rangle = \sum_{x'=1}^{x-2} \langle h(x')h(x-x'-1) \rangle. \quad (13)$$

Here, the angular brackets denote an ensemble average over all holes in the jam, and the quantity $h(x)h(u-x)$ denotes a configuration, where a hole of size x is adjacent to a hole of size $(u-x)$. The right hand side of this equation represents the rate at which holes of size x are created, and the left hand side represents the rate at which holes of size x are destroyed.

Now, we make an additional ansatz; namely, for large, x , $\langle h(x')h(x-x'-1) \rangle = G(x)$, independent of x' to leading order. That is, to leading order the probability of having two adjacent holes, whose sizes sum to x is independent of the size of either hole. $G(x)$ then also scales the same as $P_h(x)$, the probability to have a hole of size x . Thus Eq. (13), to leading order, can be written

$$\sum_{u=x}^{\infty} G(u) \sim xG(x). \quad (14)$$

Differentiating leads to

$$x \frac{\partial G(x)}{\partial x} = -2G(x); \quad G(x) \sim \frac{1}{x^2}. \quad (15)$$

Thus the distribution of hole sizes decays as

$$P_h(x) \sim x^{-\tau_h} \quad \text{with } \tau_h = 2. \quad (16)$$

It is interesting to note that the cascade equation (13) is identical to the dominant mechanism in the exact equation for forests in the one-dimensional forest fire model [34]. The exponent $\tau_h = 2$ is the same as the distribution exponent for the forests, which has been obtained exactly [35]. Curiously, $\tau_h = 2$ can also be regarded as another example of Zipf's law [36].

The exponent τ_h is related to the fractal dimension d_f of jammed vehicles by

$$\tau_h = 1 + d_f, \quad (17)$$

as long as $\tau_h \leq 2$ [37]. Thus, $\tau_h < 2$ implies that the equal time cut of the jam clusters is fractal, otherwise not. The point $\tau_h = 2$ is the boundary between fractal and dense behavior. At this special point, the random walk theory can still be expected to apply, although with logarithmic corrections.

The width of an emergent jam, at a given point in time, $w(t)$, can be expressed as

$$w(t) = \frac{n(t)}{w_j} \left[w_j + \int dx x P_h(x, t) \right]. \quad (18)$$

Here, w_j is the average width of a subjam; it is $O(1)$. The quantity $P_h(x, t)$ is the probability distribution to have a hole of size x in a jam that has survived to time t . It is natural to assume that this distribution corresponds to $P_h(x)$ up to a cutoff which grows with t . Inserting the expression for $P_h(x)$ gives

$$w(t) \sim n(t) \left[1 + \int_1^{x^*} dx x^{1-\tau_h} \right], \quad (19)$$

where the upper bound x^* represents a time-dependent cutoff. Using $\tau_h = 2$, $n \sim t^{\delta+\eta}$, and assuming $x^* \sim t^c$ gives

$$w(t) \sim t^{\delta+\eta}(1+c \ln t) \quad \text{for } \tau_h = 2. \quad (20)$$

In other words, if $\tau_h = 2$, as the above arguments suggest, spatial quantities such as $w(t)$ will exhibit logarithmic corrections to the random walk results. In the following section, we test these theoretical predictions with further numerical studies.

V. SIMULATION RESULTS

We now present the rest of our numerical results. Unless otherwise noted, these results were obtained for systems with $v_{\max} = 5$.

A. At the self-organized critical point

We study the critical properties of the outflow of a large jam by driving it with slow random perturbations as described in Sec. II. Numerically, we find (Fig. 5)

$$n(t) \equiv \langle n \rangle_{\text{surv}}(t) \sim t^{\eta+\delta}, \quad \eta + \delta = 0.5 \pm 0.1 \quad (21)$$

and (Fig. 6)

$$s(t) \sim n(t)t \sim t^{1+\eta+\delta}, \quad 1 + \eta + \delta = 1.5 \pm 0.1, \quad (22)$$

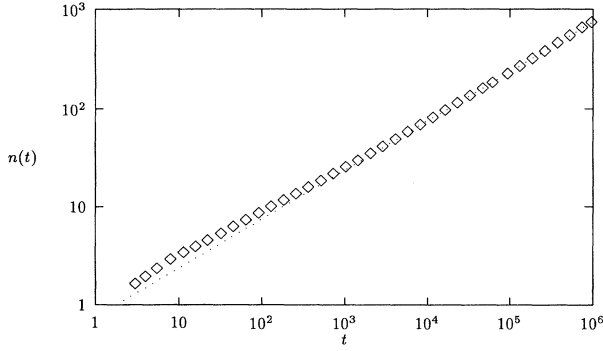


FIG. 5. Number of jammed particles at time t , $n(t)$, averaged over surviving clusters, in the outflow situation. Numerically imposed cutoff at $t = 10^6$; more than 165 000 clusters were simulated. The dotted line has slope $\frac{1}{2}$.

in agreement with the random walk predictions. However, the simulations do not converge to power law scaling before $t \approx 3 \times 10^4$, and since the simulation is cut off at $t = 10^6$, the exponents are obtained from less than two orders of magnitude in t . Figures 5 and 6 contain the averaged results of more than 160 000 avalanches, typically corresponding to approximately 200 workstation hours (see Appendix and figure captions for further information).

B. Off criticality

By changing the left boundary condition (i.e., the inflow condition) of the open system, simulations were performed both above and below the critical point. This is achieved by replacing the mega jam by the following mechanism: Vehicles are inserted with $v = v_{\max}$, at a fixed left boundary. After each vehicle, v_{\max} sites are left empty and then the following sites are attempted to be occupied with probability p_{insert} until a site is occupied. The rate p_{insert} determines an average density ρ by

$$\rho = \frac{1}{v_{\max} + 1/p_{\text{insert}}}, \quad (23)$$

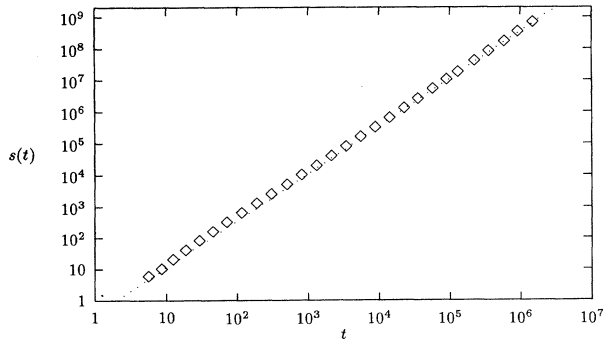


FIG. 6. Mass of jam in space time, $s(t)$, in the outflow situation, for the same clusters as in Fig. 5. Jams of similar lifetime t were averaged. The dotted line has slope $\frac{3}{2}$.

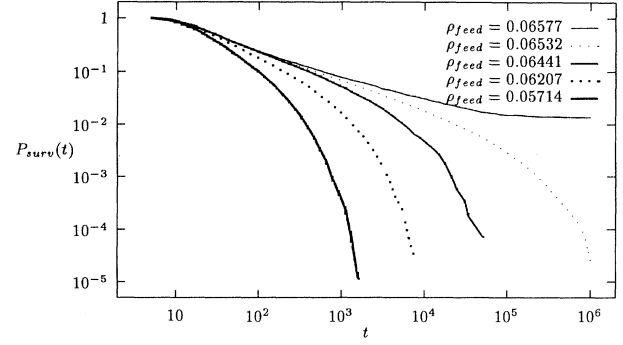


FIG. 7. Survival probability for the jam clusters, $P_{\text{surv}}(t)$, for different inflows. Note that this distribution is highly sensitive to the inflow, reconfirming that the self-organized outflow is indeed precisely critical.

which can go as high as $\rho = \rho_{\text{det,max}} = \frac{1}{6} = 0.16666\dots$ for $v_{\max} = 5$, much higher than the critical density of $\rho_c \approx 0.0655$.

We have measured the survival probability, $P_{\text{surv}}(t)$ on varying the density as shown in Fig. 7. Based on the same data, we have performed data collapse for the lifetime distribution $P(t)$ on varying the density, as shown in Fig. 8. By plotting $P/t^{-(\delta+1)}$ vs $t\Delta^{v_t}$ with the exponents $\delta+1=1.5$, $v_t=2$ was determined by the qualitatively best collapse. The accuracy of this method is not very high, though, so that the conclusion from the numerical results is no better than

$$v_t = 2 \pm 0.2, \quad (24)$$

which, again agrees with our random walk predictions.

C. Explaining previous results

These findings put us in a position to view simulation results of the original model [5] in a new context (see also [38]). In that model, multiple jams exist simultaneously. Jams start spontaneously and independently of other jams because vehicles fluctuate even at maximum speed, as determined by the parameter $p_{\text{free}} \neq 0$.

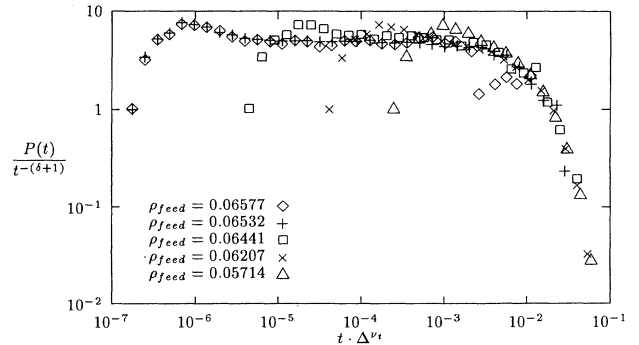


FIG. 8. Data collapse for the lifetime distribution of jams for the same data as for Fig. 7 with $\delta+1=1.5$ and $v_t=2$.

The original model displayed a scaling regime near the (self-organizing) density of maximum throughput $\rho(j_{\max})$, but with an upper cutoff at $t \approx 10^4$, which was observed to depend on p_{free} . We can now attribute this cutoff to the nonseparation of the time scales between disturbances and the emergent traffic jams. As soon as p_{free} is different from zero, the spontaneous initiation of a new jam can terminate another one. Obviously, this happens more often when p_{free} is high, which explains why the scaling region gets longer when one reduces p_{free} . Dimensional arguments suggest that the cutoff in the space-time volume, $V \sim wt$, should scale as $V_{\text{co}} p_{\text{free}} \sim 1$ (for $p_{\text{free}} \ll 1$), since this implies that a new jam is initiated in a space-time volume occupied by a previously initiated jam. According to the random walk picture $V \sim s$, so that $s_{\text{co}} \sim p_{\text{free}}^{-1}$ and $t_{\text{co}} \sim p_{\text{free}}^{-2/3}$. Measuring these correlation lengths, however, is outside of the scope of the present study.

D. Spatial behavior

So far, we have only shown simulation results for exponents describing the evolution of the number of vehicles, but not their distribution in space. Here, our simulation results are less conclusive. The width $w(t)$ vs t (Fig. 9) is, besides the convergence problems already described, best approximated by an exponent,

$$\frac{1}{z} = 0.58 \pm 0.04 \quad (25)$$

instead of $\frac{1}{2}$. Measurements of other relations (e.g., w vs n ; not shown) confirm these discrepancies for the spatial behavior of branching jam clusters with $v_{\max} > 1$. However, the form $w(t) \sim t^{1/2} \ln t$ vs t (Fig. 9) is also consistent with the numerics.

In an effort to resolve this question, we analyzed large jam configurations. We ran simulations with $v_{\max} = 2$ until a cluster reached a width of, say, $2^{13} = 8192$, and stored the configuration of this time step. About 60 configurations of the same size were used. Measuring the distribution of holes inside the configurations is consistent with the results from the cascade equation presented earlier.

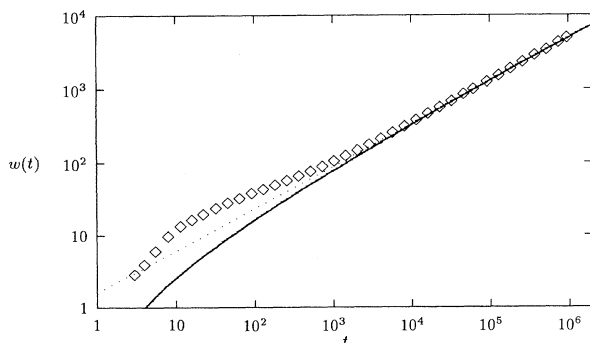


FIG. 9. Averaged maximum width of clusters, w , as a function of their lifetime, t . The dotted line has slope 0.58; the solid line is a logarithmic fit $At^{1/2} \cdot \log_{10}(t)$ where A is a free parameter.

Figure 10 shows a plot of the probability distribution for hole sizes, $P_h(x)$ vs x , obtained from these configurations. We find

$$P_h(x) \sim x^{-\tau_h}, \quad \tau_h = 1.96 \pm 0.1, \quad (26)$$

which is indeed consistent with the prediction $\tau_h = 2$ from the cascade equation.

Nevertheless, our numerical results are not precise enough to distinguish $\tau_h = 2$ from $\tau_h < 2$. Nor do our measurements for the width distinguish the power law fit with exponent 0.58 from the theoretically plausible fit with exponent $\frac{1}{2}$ and a logarithmic correction.

E. $1/f$ noise

We measured the power spectrum by first recording the time series for the number of vehicles, $N_l(t)$, in a small segment of length l in a closed system, and then taking the square of the Fourier transform:

$$S(f) = |N_l(f)|^2 = |FT[N_l(t)]|^2. \quad (27)$$

Since the jams have a finite drift velocity, the distribution of hole sizes in space is translated into the same distribution of time intervals for the activity. In particular, the hole size distribution in space translates to the first return time for jammed vehicles when sitting at a fixed position in space. It has been shown [37] that given a distribution of first return times of activity $P_{\text{first}}(t) \sim t^{-\tau_{\text{first}}}$, the power spectrum scales as $S(f) \sim 1/f^{\tau_{\text{first}}-1}$. Using the result $\tau_h = \tau_{\text{first}} = 2$ this gives precisely a $1/f$ power spectrum for the noise. The power spectrum for the original model with the parameter $p_{\text{free}} = 0.5, 0.005, 0.00005$ was measured in a closed system near the critical density. As shown in Fig. 11, the numerical results are in general agreement with this prediction. This result agrees qualitatively with the power spectrum results for granular flow both in experiments [17,13] and in simulations [14–16], and offers an alternative explanation for $1/f$ noise observed in traffic flow [39,40].

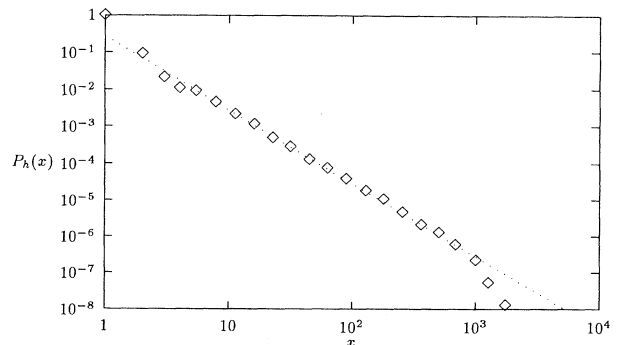


FIG. 10. Probability distribution P_h for hole sizes x . The dotted line has slope -2 . The average is over 60 configurations, which all have width $w = 2^{13}$. Contrary to all other figures in this chapter, these results were obtained with $v_{\max} = 2$.

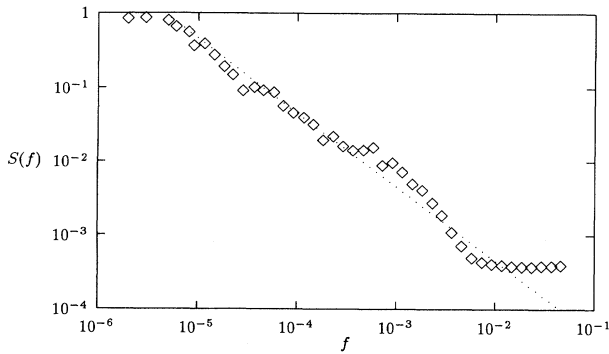


FIG. 11. Power spectrum, $S(f)$, smoothed by averaging, for a closed system of length $L = 10^5$ and with $p_{\text{free}} = 0.00005$. Dotted line has slope -1 .

VI. APPLICATIONS TO REAL TRAFFIC

With respect to real world traffic, much of this discussion appears rather abstract. A configuration of size $2^{13} = 8192$, as analyzed in this work, corresponds to more than 100 km of undisturbed roadway, a situation that rarely occurs in reality. However, the following results should be general enough to be important for traffic.

(i) The concept of critical phase transitions is helpful for characterizing real traffic behavior. Open systems will tend to go close to a critical state that is determined by the outflow from large jams. This underlying self-organized critical state corresponds to a percolative transition for the jams; i.e., spontaneous small fluctuations can lead to large emergent traffic jams.

(ii) Interestingly, planned or already installed technological advancements such as cruise-control or radar-based driving support will tend to reduce the fluctuations at maximum speed similar to our limit, thus increasing the range of validity of our results. One unintended consequence of these flow control technologies is that, if they work, they will in fact push the traffic system closer to its underlying critical point; thereby making prediction, planning, and control more difficult.

(iii) The fact that traffic jams are close to the border of fractal behavior means that, from a single “snapshot” of a traffic system, one will not be able to judge which traffic jams come from the same “reason.” Concepts like queues [41] or single waves do not make sense when traffic is close to criticality. “Phantom” traffic jams emerge spontaneously from the dynamics of branching jam waves.

The fact that holes scale with an exponent around -2 means that, at criticality, the jammed cars are close to not carrying any measure at all. The regime near maximum throughput thus corresponds to large “holes” operating practically at ρ_c and j_{max} , plus a network of branched jam clusters, which do not change ρ and j very much. The fluctuations found in the 5-min measurements of traffic at capacity [49] therefore reflect the fact that traffic flow is inhomogeneous with essentially two states (jammed and maximum throughput). The result of each 5-min measurement depends on how many jam branches are measured during this period.

APPENDIX A: COMPUTATIONAL STRATEGIES AND PROBLEMS

Computationally, we use a “vehicle-oriented” technique for most of the results presented here. Vehicles are maintained in an ordered list, and each vehicle has an integer position and an integer velocity. Since we model single-lane traffic, passing is impossible, and the list always remains ordered.

We simulate a system which is, for all practical purposes, infinite in space. The idea is comparable to a Leath algorithm in percolation [42], which also only remembers the active part of the cluster.

As we described earlier, a jam cluster is surrounded by deterministic traffic. Let us assume that the leftmost car of this jam has the number i_{eff} and is at position x_{left} (similar for the rightmost car). Cars are numbered from left to right; traffic is flowing from left to right.

To the right of car i_{right} , everything is deterministic and at maximum speed, and, in consequence, nothing happens which can influence the jam. Therefore, we do not change the properties of the jam if we do not simulate these cars. Moreover, as soon as car i_{right} becomes deterministic, it can never reenter the nondeterministic regime. Therefore, car number $i_{\text{right}} - 1$ becomes the new rightmost car, and car number i_{right} is no longer considered for the simulation.

To the left of car i_{left} , the situation is similar. The only information that we need is the sequence of the gaps (n_{gap_i}) of the incoming cars. Just before car $i_{\text{left}} - 1$ enters the jam, we add one more car to the left, with $n_{\text{gap}_{i_{\text{left}}-2}}$.

It is obvious that, with this computational technique, the only restriction for the spatial size is given by the memory of the computer. Since our model is one dimensional, this has never been a problem.

A remaining question is how to obtain the sequence of gaps (n_{gap_i}) of the incoming cars, especially for the outflow situation. One possibility would be to first run another simulation of the outflow from a megajam. Cars leave this megajam, drive through a regime of decreasing density, and eventually relax to the deterministic state. One then records the gaps between these cars, writes them to a file, and reads this file during the other simulation. Apart from technicalities (avoiding the intermediate file), this is the technique we adopted in our simulations.

Our program runs with approximately 270 000 vehicle updates per second on a SUN-Sparc10 workstation; and since the critical density is $\rho_c \approx 0.0655$, for $v_{\text{max}} = 5$ this corresponds to $270\,000/0.0655 = 4.1 \times 10^6$ site updates per second. This includes all time for measurements and for the production of the gaps of the incoming cars.

We showed that our numerical results cannot resolve the question between logarithmic corrections for the width $w(t)$ or an exponent different from $\frac{1}{2}$, in spite of data obtained over six orders of magnitude in time. The reason for this is a large “bump” in the measurements of the width. Simulations of larger systems would have been helpful. The time complexity for our questions is

$O(t)$: As shown above, when averaging over all started clusters, the number of active sites, $\langle n \rangle_{\text{started}}$, is constant in time: $\langle n \rangle_{\text{started}}(t) \sim t^0$. When t_{co} is the numerically imposed cutoff, then we perform for each started cluster in the average αt_{co} updates of a vehicle. In our experience, $\alpha \approx 5$ for $v_{\text{max}} = 5$.

In order words, in order to add another order of magnitude in time, with the same statistical quality as before, we would need a factor of 10 more computational power. However, each of our graphs already stems from runs using 4 or more Sparc10 workstations for 10 days or more. And using a parallel supercomputer seems difficult: Standard geometric parallelization is ineffective because most of the time the jam clusters are quite small, and in consequence all the CPU's responsible for cars further away

“from the middle of the jam” would be idle. More sophisticated load-balancing methods might be a solution.

ACKNOWLEDGMENTS

This work was supported by the U.S. Department of Energy Division of Materials Science, under contract DE-AC02-76CH00016. M.P. thanks the U.S. Department of Energy Distinguished Postdoctoral Research Program, K.N. the “Graduiertenkolleg Scientific Computing Köln/St. Augustin” for financial support. We thank Sergei Maslov, Per Bak, Sergei Esipov, Chris Caplice, and Oh-Kyoung Kwon for useful discussions. K.N. thanks Brookhaven National Laboratory and Los Alamos National Laboratory for their hospitality. The “Zentrum für Paralleles Rechnen” ZPR Köln provided most of the computer time.

-
- [1] Eno Foundation for Transportation, *Transportation in America* (Transportation Policy Associates, Washington, D.C., 1992); Contained in National Transportation Statistics, D.O.T. Report No. DOT-VNTFC-RSPA-92-1, 1992 (unpublished).
- [2] O. Biham, A. Middleton, and D. Levine, *Phys. Rev. A* **46**, R6124 (1992).
- [3] M. Takayasu and H. Takayasu, *Fractals* **1**, 860 (1993); J. Schafer and D. E. Wolf, *Phys. Rev. E* (in press).
- [4] K. Nagel and M. Schreckenberg, *J. Phys. I (France)* **2**, 2221 (1992).
- [5] K. Nagel, *Int. J. Mod. Phys. C* **5**, 567 (1994).
- [6] R. Kühne, in *Highway Capacity and Level of Service*, edited by U. Brannolte, Proceedings of the International Symposium on Highway Capacity in Karlsruhe (Rotterdam, Balkema, 1991).
- [7] B. S. Kerner and P. Konhäuser, *Phys. Rev. E* **50**, 54 (1993).
- [8] D. Helbing (unpublished).
- [9] F. L. Hall, B. L. Allen, and M. A. Gunter, *Trans. Res. A* **20**, 197 (1986).
- [10] I. Treiterer and J. A. Myers, *International Symposia on Transportation and Traffic Theory*, edited by D. J. Buckley (A. H. & A. W. Reed Pty Ltd., New South Wales, 1974).
- [11] P. Bak, C. Tang, and K. Wiesenfeld, *Phys. Rev. A* **38**, 368 (1988).
- [12] H. M. Jaeger and S. R. Nagel, *Science* **255**, 1523 (1992), and references therein.
- [13] G. W. Baxter, R. P. Behringer, T. Fagert, and G. A. Johnson, *Phys. Rev. Lett.* **62**, 2825 (1989).
- [14] G. Ristow and H. J. Herrmann, *Phys. Rev. E* **50**, R5 (1994).
- [15] G. Peng and H. J. Herrmann, *Phys. Rev. E* **48**, R1796 (1994).
- [16] G. Peng and H. J. Herrmann (unpublished).
- [17] K. L. Schick and A. A. Verveen, *Nature* **251**, 599 (1974).
- [18] S. F. Shandarin and Y. B. Zeldovich, *Rev. Mod. Phys.* **61**, 185 (1989); L. Pietronero, *Physica A* **144**, 257 (1987).
- [19] I. Goldhirsch and G. Zanetti, *Phys. Rev. Lett.* **70**, 1619 (1993); Y. Du, H. Li, and L. P. Kadanoff (unpublished).
- [20] W. Leutzbach, *Introduction to the Theory of Traffic Flow* (Springer, Berlin, 1988).
- [21] R. Wiedemann, *Simulation des Straßenverkehrsflusses*, Schriftenreihe des Instituts für Verkehrswesen der Universität Karlsruhe, Heft 8 (1974).
- [22] For clarity, $N_f + N_j = N$, $L_f + L_j = L$, $N_f/L_f = 1/a$, $N_j/L_j = \rho_c$, where N_f, L_f , and ρ_c are the number, length, and density, respectively, in the free flowing phase, and N_j, L_j , and $1/a$ are the corresponding quantities in the jammed phase.
- [23] M. Bando, K. Hasebe, A. Nakayama, A. Shibata, and Y. Sugiyama, *Jpn. Appl. Math.* **11**, 203 (1994).
- [24] J. M. Carlson, J. T. Chayes, E. R. Grannan, and G. H. Swindle, *Phys. Rev. Lett.* **65**, 2547 (1990).
- [25] J. Krug, in *Spontaneous Formation of Space-time Structures and Criticality*, edited by T. Riste and D. Sherrington (Kluwer Academic, Netherlands, 1991).
- [26] B. Derrida, E. Domany, and D. Mukamel, *J. Stat. Phys.* **69**, 667 (1992).
- [27] K. Nagel and H. J. Herrmann, *Physica A* **199**, 254 (1993).
- [28] A. Kanaan (private communication).
- [29] B. B. Mandelbrot, *The Fractal Geometry of Nature* (Freeman, New York, 1983).
- [30] P. Grassberger and A. de la Torre, *Ann. Phys. (N.Y.)* **122**, 373 (1979).
- [31] M. Bramson and L. Gray, *Z. Warsch. Gebiete* **68**, 3060 (1985).
- [32] I. Jensen and R. Dickman, *Phys. Rev. E* **48**, 1710 (1993).
- [33] W. Feller, *An Introduction to Probability Theory and Its Applications* (Wiley, New York, 1968) Vol. 1.
- [34] M. Paczuski and P. Bak, *Phys. Rev. E* **48**, R3214 (1993).
- [35] B. Drossel, S. Clar, and F. Schwabl, *Phys. Rev. Lett.* **71**, 3739 (1993).
- [36] G. K. Zipf, *Human Behavior and the Principle of Least-Effort* (Addison-Wesley, Cambridge, 1949); see, for example, M. Gellman, *The Quark and the Jaguar* (Freeman, New York, 1994).
- [37] S. Maslov, M. Paczuski, and P. Bak, *Phys. Rev. Lett.* **73**, 2162 (1994).
- [38] K. Nagel and S. Rasmussen, in *Proceedings of Alife 4*, edited by R. Brooks and P. Maes (MIT Press, Cambridge, 1994).
- [39] T. Musha and H. Higuchi, *Jpn. J. Appl. Phys.* **15**, 1271 (1976).
- [40] T. Musha and H. Higuchi, *Jpn. J. Appl. Phys.* **17**, 811 (1978).
- [41] H. P. Simão and W. B. Powell, *Trans. Sci.* **26**, 296 (1992).
- [42] P. L. Leath, *Phys. Rev. B* **14**, 5046 (1976).